Channel interference in resonant Auger scattering by surface adsorbed molecules

Faris Gel'mukhanov*
Institute of Physics and Measurement Technology, Linköping University, S-581 83, Linköping, Sweden

Vincenzo Carravetta
Istituto di Chimica Quantistica ed Energetica Molecolare del CNR, Via Risorgimento 35, 56100 Pisa, Italy

Hans Ågren
Institute of Physics and Measurement Technology, Linköping University, S-581 83, Linköping, Sweden
(Received 12 January 1998)

We present theory of resonant Auger scattering in gas-phase and surface-adsorbed molecules focusing on the role of channel interference. The connections between parity selection rules, parity of the Auger electron wave functions, Bragg conditions, and channel interference are uncovered. The channel interference is found sensitively dependent on the phase factors of the Auger electron and the incident x-ray photons, something that makes the scattering cross sections strongly anisotropic and oscillatory. Parity selection rules are found that apply to a fairly broad class of molecules, but which can be violated by different dephasing mechanisms that destroy the coherence. The parity-selection rules are particularly sensitive to the degree of orientational disorder of the molecules, something that actually can be used for investigations of adsorbate orientation. Three types of coherence destroying, dephasing mechanisms are investigated: orientational disorder, vibrational and librational motion, and scattering of the emitted electron by the surrounding atoms. It is predicted that the selection rules can be obstructed by thermal vibrations and librations even at very low temperature due to the zero-point contributions. The selection rules and the dephasing mechanisms are explored for one-, two-, and three-dimensional adsorbate systems. [S0163-1829(98)03928-9]

I. INTRODUCTION

Over the past decade studies of radiative and nonradiative resonant x-ray Raman scattering (RXS) have been carried out for a wide variety of molecules in the gas phase[1–5] and in physisorbed or chemisorbed states[6,4,7,8] by using tunable narrow band-pass polarized synchrotron radiation. With increased overall quality and resolution of the spectra it has been possible to utilize the selection rules as an interpretational tool for radiative RXS spectra.[9,10,1] On the other hand, selection rules are uncommon in nonradiative RXS (or resonant Auger Raman), owing mainly to the fact that the decay Coulomb operator is more complex than the dipole operator and that the continuum Auger electron wave-function in general lacks molecular symmetry. The consequence of these facts is that a great number of the resonances are observed in the resonant Auger spectra. There is a deep connection between selection rules and interference of the scattering channels through the core hole states localized at different identical atoms in the radiative case.[9,11] It seems probable that channel interference is important also in resonant Auger scattering of symmetrical systems, and that one can find connections between interference and selection rules also for that spectroscopy.

The purpose of the present paper is to give a general analysis of the channel interference in resonant Auger scattering (RAS) by symmetrical systems. We investigate the existence of parity selection rules in RAS in specific conditions, and show that the manifestation of such rules is very sensitive to the degree of orientational disorder of the molecules. General three-dimensional disorder is considered, as well as one- and two-dimensional ordering that is possible for physisorbed or chemisorbed molecules.[12] Like for radiative RXS,[9] the RAS cross section shows characteristic interference oscillations due to the indistinguishability of the scattering channels through the core excited states localized at different identical atoms. However, in contrast to radiative RXS these oscillations are caused by channel interference induced by phase factors of both the incident x-ray photon and the ejected high-energy Auger electron. These interference oscillations provide structural information. The large value of the Auger electron momentum leads to interference oscillations even in the soft x-ray region. The selection rules in RAS are a direct consequence of the coherence of the scattering channels through core-excited states localized at different atoms. Any dephasing mechanism destroying this coherence leads, therefore, to violations of the parity selection rules. We investigate three types of such dephasing mechanisms: orientational disorder, vibrational and librational motion, and scattering of emitted electrons by surroundings atoms.

This paper is organized as follows: Following this introduction, Sec. II is devoted to the phase analysis of the RAS amplitude where both the photon and Auger electron phases are accounted for. In Sec. III we derive parity selection rules and show the deep connection between selection rules and Bragg conditions. To give insight into the physics of the selection rules, we discuss in Sec. III C the parity properties of the wave functions of both the x-ray photon and the Auger electron. This section shows the remarkable connection between the angular distribution of the Auger electron parity and that of the RAS cross section. The violation of the parity

selection rules due to the orientational disorder of the molecules is discussed in Sec. IV. The breakdown of the parity selection rules by vibrational and librational dephasing is considered in Sec. V A. In Sec. VI we discuss the diffractional scattering of Auger electrons by surrounding atoms, which also can mask the observation of selection rules. A short analysis of the experimental possibilities for observation is finally given in Sec. VII. Atomic units are used unless otherwise stated.

II. PHASE ANALYSIS OF SCATTERING AMPLITUDE

We begin by deriving a theory for the special case of resonant Auger scattering by a homonuclear diatomic molecule A_2, which reflects most aspects of the general case but at the same time allows a tractable presentation. The energy ω of x-ray photons with wave vector $\mathbf{p}$ and polarization vector $\mathbf{e}$ is passed, during the scattering, to the Auger electron of energy $\varepsilon = k^2/2$ and momentum $\mathbf{k}$ and to the remaining molecular ion excited to the final electronic state $|f\rangle$. According to the Fermi golden rule, the double differential RAS cross section for a fixed molecular orientation and finite band-pass excitation is given by[2,9]

$$\sigma_f(\epsilon,\omega) = |F|^2 \Phi(\omega + E_o - \epsilon - E_f, \gamma), \tag{1}$$

where E_o and E_f are the energies of the ground and final ionic molecular states, respectively. The lifetime broadening of the final state Γ_f is often small in comparison with the lifetime broadening Γ of the core excited states and in comparison with the width γ of the spectral function $\Phi(\omega' - \omega, \gamma)$ of the incident radiation. Therefore, Γ_f is neglected in Eq. (1).

For the analysis of the phase we consider only the resonant part of the RAS amplitude[2,9,13] that gives, by far, the most important contribution. Since the atoms (enumerated as 1 and 2) in the A_2 molecule cannot be distinguished, we must take into account the scattering from both atoms. In other words, the RAS amplitude F can be seen as the sum of two partial scattering amplitudes

$$F = F_1 + F_2, \quad F_i \propto \frac{Q_{fi}(\mathbf{k})(\mathbf{e}\cdot\mathbf{D}_{io}) e^{i\mathbf{p}\cdot\mathbf{R}_i}}{\epsilon - \omega_{if} - i\Gamma}. \tag{2}$$

Here, $\mathbf{R}_i$ is the radius vectors of the atom $i=1,2$, $\mathbf{D}_{io}$ is the dipole moment of the photoabsorption transition $o \to i$, while Q is the Coulomb operator of the Auger decay transition. We choose here a localized representation for the core excited states with the dipole and Coulomb matrix elements evaluated at the two core-hole sites (in the following a detailed discussion is given of the dipole approximation here adopted). The resonance energy $\omega_{if} = E_i - E_f$ of the Auger transition from the core excited $|i\rangle$ to the final ionic state $|f\rangle$ does not depend on the core-hole site. The RXS amplitude is invariant relative to the choice of representation for the core excited states due to the degeneracy of the core shells in a homonuclear diatomic molecule.[9]

We will consider the case of high-energy Auger electrons, which allows us to express, in a first approximation, the Auger electron wave functions $\psi_{\mathbf{k}}(\mathbf{r})$ relative to the nucleus i as

$$\psi_{\mathbf{k}}(\mathbf{r}) = \psi_{\mathbf{k}i}(\mathbf{r} - \mathbf{R}_i) e^{i\mathbf{k}\cdot\mathbf{R}_i}, \tag{3}$$

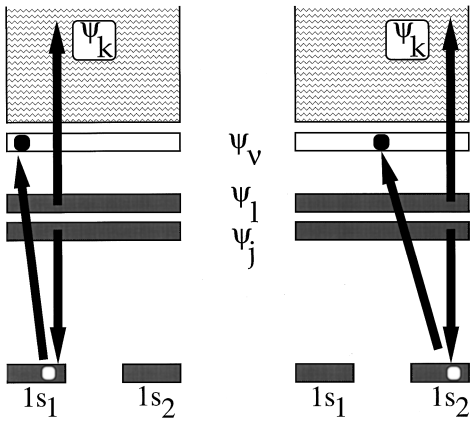

FIG. 1. Scheme of spectral transitions.

where $\psi_{\mathbf{k}i}(\mathbf{r} - \mathbf{R}_i)$ is the solution of the Schrödinger equation close to the ith atom. The applicability of this high-energy approximation will be discussed in detail in Sec. VI.

A. Phase and symmetry of the Coulomb matrix element

Without loss of generality let us analyze the spectator scheme of resonant Auger scattering (Fig. 1) with photoexcitation $1s_i \to \psi_\nu$ and the subsequent decay transition: $\psi_j \to 1s_i$, $\psi_l \to \psi_{\mathbf{k}}$ (the corresponding exchange channel is $\psi_l \to 1s_i$, $\psi_j \to \psi_{\mathbf{k}}$). The decay matrix element Q_{fi} consists of two terms that, in the independent-particle approximation for initial and final states, can be expressed as

$$Q_{fi}(\mathbf{k}) = (\psi_{\mathbf{k}}\psi_l|\psi_j 1s_i) + \eta(\psi_{\mathbf{k}}\psi_j|\psi_l 1s_i), \tag{4}$$

$$(\psi_{\mathbf{k}}\psi_l|\psi_j 1s_i) \equiv \int \psi^*_{\mathbf{k}}(\mathbf{r}_1)\psi_l(\mathbf{r}_1)\frac{1}{r_{12}}\psi_j(\mathbf{r}_2)1s_i(\mathbf{r}_2)d\mathbf{r}_1 d\mathbf{r}_2.$$

The dimensionless parameter η depends on the total spin and electronic configuration of the final state.[14] To emphasize the symmetry of the molecular orbital (MO) ψ_j, we will write it in terms of the atomic contributions ϕ_{j1} and ϕ_{j2} according to

$$\psi_j = c_{j1}\phi_{j1} + c_{j2}\phi_{j2}, \quad \phi_{ji} \equiv \phi_j(\mathbf{r} - \mathbf{R}_i), \quad c_{j2} = \pm c_{j1}. \tag{5}$$

In the following (except in Sec. III C) we will assume that both ψ_j and ψ_l are π MO's consisting of mainly p atomic orbitals. The importance of this assumption will be clarified in Sec. III C. With the above expression for the Coulomb matrix element and Eq. (3), we then obtain

$$Q_{f1}(\mathbf{k}) \simeq c_{j1}c_{l1}(1+\eta)g_{\mathbf{k}}e^{-i\mathbf{k}\cdot\mathbf{R}_1} + (c_{j1}c_{l2} + \overline{\eta}c_{j2}c_{l1})\overline{g}_{\mathbf{k}}e^{-i\mathbf{k}\cdot\mathbf{R}_2}. \tag{6}$$

In addition, we assume a small two-center overlap $\phi_{j2}1s_1$ and that the atomic p orbitals ϕ_{li} and ϕ_{ji} are the same. The expression for the Coulomb matrix element $Q_{f2}(\mathbf{k})$ is given by Eq. (6) after replacement $1 \rightleftharpoons 2$. The one-center $g_{\mathbf{k}}$ and two-center $\overline{g}_{\mathbf{k}}$ Coulomb integrals are defined as

$$g_{\mathbf{k}} = (\psi_{\mathbf{k}1}\phi_{l1}|\phi_{j1}1s_1), \quad \overline{g}_{\mathbf{k}} = (\psi_{\mathbf{k}2}\phi_{l2}|\phi_{j1}1s_1). \tag{7}$$

For brevity we redefined in Eq. (6) the parameter η of Eq. (4) according to $\eta \rightarrow \eta g_{\mathbf{k}}^{\mathrm{exc}}/g_{\mathbf{k}}$, $\overline{\eta} \rightarrow \eta \overline{g}_{\mathbf{k}}^{\mathrm{exc}}/\overline{g}_{\mathbf{k}}$. The exchange integrals $g_{\mathbf{k}}^{\mathrm{exc}}$ and $\overline{g}_{\mathbf{k}}^{\mathrm{exc}}$ are given by the expression for direct Coulomb integrals $g_{\mathbf{k}}$ and $\overline{g}_{\mathbf{k}}$ (7) after replacement $l \rightleftharpoons j$.

The photon and electron phase factors $\exp(\pm \mathbf{p}\mathbf{R}_i)$ and $\exp(\pm \mathbf{k}\mathbf{R}_i)$ in the final expression of the scattering amplitude,

$$F \propto \frac{(\mathbf{e}\cdot\mathbf{d}_\nu)}{\epsilon-\omega_{if}-i\Gamma}\,[c_{\nu 1}Q_{f1}(\mathbf{k})e^{i\mathbf{p}\cdot\mathbf{R}_1}+c_{\nu 2}Q_{f2}(\mathbf{k})e^{i\mathbf{p}\cdot\mathbf{R}_2}], \tag{8}$$

reflect the coherence properties of the scattering channels through the first ($i=1$) and second ($i=2$) identical atoms of the A_2 molecule. Here $\mathbf{d}_\nu = \langle \phi_{\nu 1}|\mathbf{r}|1s_1\rangle = \langle \phi_{\nu 2}|\mathbf{r}|1s_2\rangle$ is the atomic dipole-matrix element.

B. Auger decay rate vs symmetry

There is an infinite degeneracy of the unbound wave functions at any energy in the molecular continuum, corresponding to the infinite number of possible propagation directions. As a consequence, the continuum orbital of the Auger electron $\psi_{\mathbf{k}}(\mathbf{r})$ in Eq. (3) has, in contrast to the the bound MO's no definite parity with respect to inversion relative to the molecular center. The Auger electron wave function close to the ith atom [Eq. (3)] can, in fact, be decomposed into contributions of opposite parity (for inversion at center i)

$$\psi_{\mathbf{k}i} = \psi_{\mathbf{k}i}^{\mathrm{even}} + \psi_{\mathbf{k}i}^{\mathrm{odd}}. \tag{9}$$

The *even* ($\psi_{\mathbf{k}i}^{\mathrm{even}}$) and *odd* parts ($\psi_{\mathbf{k}i}^{\mathrm{odd}}$) are the sums of terms proportional to spherical harmonics [$Y_{\mathrm{LM}}(\hat{\mathbf{r}}_i)$] with even and odd orbital momenta L, respectively. This fact and the symmetry analysis of the atomic Coulomb integrals [Eq. (7)] lead immediately to the result that, in general, Auger decay to both even and odd continuum states $\psi_{\mathbf{k}i}^{\mathrm{even}}$ and $\psi_{\mathbf{k}i}^{\mathrm{odd}}$, and no parity selection rule applies to the RAS cross section.

However, the situation changes qualitatively when both the MO's ψ_l and ψ_j involved in the Auger decay can be expressed in terms of atomic orbitals ϕ_{ji}, which have the same definite parity (*even* or *odd*) for inversion at center i. This is, for instance, the case of π orbitals with negligible contributions from d orbitals. Now only the even harmonics of the Auger orbital

$$\psi_{\mathbf{k}i} = \psi_{\mathbf{k}i}^{\mathrm{even}} \tag{10}$$

contribute to the Coulomb integrals in Eq. (7). This assumption, which also will be made in the following, applies to a fairly extensive number of molecules.

III. PARITY SELECTION RULES AND CHANNEL INTERFERENCE

The experimentally measured quantity, the RAS cross section (1), can be written in the following way:

$$\begin{aligned}\sigma_f(\epsilon,\omega) = a|(\mathbf{e}\cdot\mathbf{d})g_{\mathbf{k}}|^2\,\frac{\Phi(\omega+E_o-\epsilon-E_f,\gamma)}{(\epsilon-\omega_{if})^2+\Gamma^2}\\ \times(\mathcal{A}\{1-\mathcal{P}_f\cos[(\mathbf{k}-\mathbf{p})\cdot\mathbf{R}]\}\\ +\mathcal{B}\{1-\mathcal{P}_f\cos[(\mathbf{k}+\mathbf{p})\cdot\mathbf{R}]\}\\ +\mathcal{C}[\cos(\mathbf{p}\cdot\mathbf{R})-\mathcal{P}_f\cos(\mathbf{k}\cdot\mathbf{R})]),\end{aligned} \tag{11}$$

where

$$\mathcal{A}=(1+\eta)^2,\quad \mathcal{B}=\left|\frac{\overline{g}_{\mathbf{k}}}{g_{\mathbf{k}}}\right|^2(1+\overline{\eta}^2+2\mathcal{P}_j\mathcal{P}_l\overline{\eta}),$$

$$\mathcal{C}=2\left|\frac{\overline{g}_{\mathbf{k}}}{g_{\mathbf{k}}}\right|(1+\eta)(\mathcal{P}_l+\mathcal{P}_j\overline{\eta})\mathcal{P}_f\cos\varphi, \tag{12}$$

$\mathbf{R}=\mathbf{R}_2-\mathbf{R}_1$, $a\propto 2(c_{\nu 1}c_{l1}c_{j1})^2$, φ is the phase of product $g_{\mathbf{k}}\overline{g}_{\mathbf{k}}^*$: $g_{\mathbf{k}}\overline{g}_{\mathbf{k}}^* = |g_{\mathbf{k}}\overline{g}_{\mathbf{k}}|\exp(i\varphi)$, and assuming here a gerade ground state.

We take into account here the parity of the orbitals with respect to the center of the homonuclear diatomic molecule by the quantity $\mathcal{P}_j = -\mathrm{sgn}(c_{j1}c_{j2}) = \pm 1$ for the MO ψ_j. The positive sign of $\mathcal{P}_j$ corresponds to ψ_j gerade, while the minus sign corresponds to ψ_j ungerade. Assuming a gerade ground state, $\mathcal{P}_f = \mathcal{P}_\nu\mathcal{P}_j\mathcal{P}_l$ will then describe the parity of the many-electron final-state wave function of the ion A_2^+ ($\mathcal{P}_f=+1$ for gerade final state and vice versa).

A. Bragg and soft x-ray limits

The cosines on the right-hand side of Eq. (11) describe the interchannel interference deriving from the x-ray photon and Auger electron-phase factors. This interference is very parity sensitive. To make this statement more clear we consider the case when the photon interference factor $\mathbf{p}\cdot\mathbf{R}$ satisfies the Bragg condition

$$\mathbf{p}\cdot\mathbf{R} = n\pi, \tag{13}$$

where n is an integer. Now the RAS cross section (11) takes the strikingly simple form

$$\sigma_f(\epsilon,\omega) = \sigma_o(\hat{\mathbf{R}})[1-(-1)^n\mathcal{P}_f\cos(\mathbf{k}\cdot\mathbf{R})] \tag{14}$$

with

$$\begin{aligned}\sigma_o(\hat{\mathbf{R}}) = a|(\mathbf{e}\cdot\mathbf{d}_\nu)g_{\mathbf{k}}|^2\,\frac{\Phi(\omega+E_o-\epsilon-E_f,\gamma)}{(\epsilon-\omega_{if})^2+\Gamma^2}\\ \times[\mathcal{A}+\mathcal{B}+(-1)^n\mathcal{C}],\end{aligned} \tag{15}$$

and $\hat{\mathbf{R}} \equiv \mathbf{R}/R$ as unit vector parallel to $\mathbf{R}$. The case with $n=0$ corresponds to the case of soft x rays $|\mathbf{p}\cdot\mathbf{R}| \ll 1$ or to the case of propagation of the x rays in a direction perpendicular to the molecular axis. A similar result is obtained when the Bragg condition (13) is fulfilled by the Auger electron interference factor

$$\mathbf{k}\cdot\mathbf{R} = n'\pi \tag{16}$$

with integer n'. It is sufficient to perform the following replacements: $\cos(\mathbf{k}\cdot\mathbf{R}) \rightarrow \cos(\mathbf{p}\cdot\mathbf{R})$ in Eq. (14) and $\mathcal{C} \rightarrow \mathcal{P}_f\mathcal{C}$ in Eq. (15). Figure 2 gives the cross section as a function of the

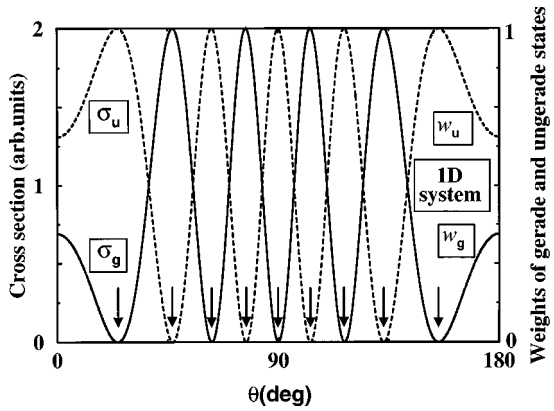

FIG. 2. *1D ordering.* Partial RAS cross sections $\overline{\sigma_g}(\epsilon,\omega)$, $\overline{\sigma_u}(\epsilon,\omega)$ [Eqs. (28) and (27)] and weights w_g, w_u [Eq. (27)] of the gerade and ungerade final states, respectively. The case of soft x rays ($n=0$) and identical molecular orientations [Eq. (30)]. θ is the angle between **k** and the molecular axis. The arrows mark the angles where the parity-selection rules take place. $kR=14$ is the value of the interference parameter for O_2.

angle between **k** and **R**. It shows that the gerade and ungerade final states correspond to interference patterns of opposite phase.

B. Parity selection rules

Strict parity selection rules are obtained when both $\mathbf{k}\cdot\mathbf{R}/\pi$ and $\mathbf{p}\cdot\mathbf{R}/\pi$ are integers:

$$\sigma_f(\epsilon,\omega)=0 \quad \text{if } f=\begin{cases} g, & \dfrac{(\mathbf{k}+\mathbf{p})\cdot\mathbf{R}}{\pi}=\text{even} \\ u, & \dfrac{(\mathbf{k}+\mathbf{p})\cdot\mathbf{R}}{\pi}=\text{odd.} \end{cases} \tag{17}$$

C. Parity of photon and Auger electron wave functions and the Bragg condition

The origin of the selection rules in Eq. (17) can be understood by an elementary, albeit physically deeper, analysis of the scattering process. It is evident that the parity selection rules for the scattering amplitude

$$F\propto\langle o,\text{photon}|(\mathbf{e}\cdot\mathbf{D}|i\rangle\langle i|Q|F,\text{Auger electron}\rangle \tag{18}$$

must follow from the general selection rule

$$\mathcal{P}_o\otimes\mathcal{P}(\text{photon})\otimes\mathcal{P}(\mathbf{D})\otimes\mathcal{P}(\text{Auger electron})\otimes\mathcal{P}_f=\text{ungerade} \tag{19}$$

with the gerade Coulomb operator Q. This condition of $F=0$ is nothing else than the requirement of ungerade parity of the integrand in the general expression for the scattering amplitude (18). The left-hand side of Eq. (19) is just the product of the parities of all the factors of the scattering amplitude. They are as follows: the parities of the ground and final molecular states ($\mathcal{P}_o$ and $\mathcal{P}_f$, respectively); the ungerade parity $\mathcal{P}(\mathbf{D})$ of the dipole moment; the parity of the incident x-ray photon $\mathcal{P}$(photon), and the parity of the Auger electron $\mathcal{P}$(electron).

Here one principal point deserves comment. Contrary to molecular-bound ground and final states, the wave functions of photon $\psi^{\text{ph}}(\mathbf{r})=\mathbf{e}\cdot\exp(i\mathbf{p}\cdot\mathbf{r})$ and Auger electron $\psi_{\mathbf{k}}(\mathbf{r})$ have no certain parities in the general case. However, under some conditions the notion of parity may still be defined, as, for example, at shape resonances where the continuum wave function of the photoelectron can have a well-defined symmetry.[15–17]

We consider the photon wave function in a form reflecting the locality of the x-ray photoabsorption process by the molecule A_2. Due to the localization of the $1s$ atomic orbitals (of the size a_{1s}) the core photoabsorption selects the following fraction of the photon wave function:

$$\psi^{\text{ph}}(\mathbf{r})\propto e^{i\alpha}(\psi_1^{\text{ph}}+e^{i\mathbf{p}\cdot\mathbf{R}}\psi_2^{\text{ph}}), \tag{20}$$

where $\alpha=\mathbf{p}\cdot\mathbf{R}_1$. ψ_i^{ph} differs from zero ($\psi_i^{\text{ph}}=\psi^{\text{ph}}(\mathbf{r}-\mathbf{R}_i)=\mathbf{e}\cdot\exp[i\mathbf{p}(\mathbf{r}-\mathbf{R}_i)]$) only in the region of the $1s$ wave function of the ith atom. We can then here use the dipole approximation for the inner atomic transition because $pa_{1s}\ll 1$. This implies a ''local'' even parity of the photon wave function close to both atoms 1 and 2,

$$\psi_i^{\text{ph}}=\mathbf{e}\times\begin{cases}1, & r_i<a_{1s}\\ 0, & r_i>a_{1s},\end{cases} \tag{21}$$

where $\mathbf{r}_i=\mathbf{r}-\mathbf{R}_i$. The parity properties of the photon wave function with respect to the inversion center of the molecule can be seen if we rewrite $\psi^{\text{ph}}(\mathbf{r})$ as

$$\psi^{\text{ph}}(\mathbf{r})\propto e^{i(\alpha+\mathbf{p}\cdot\mathbf{R}/2)}\left[\cos\left(\frac{\mathbf{p}\cdot\mathbf{R}}{2}\right)\psi_g^{\text{ph}}-i\,\sin\left(\frac{\mathbf{p}\cdot\mathbf{R}}{2}\right)\psi_u^{\text{ph}}\right] \tag{22}$$

in terms of the gerade and ungerade functions, $\psi_{g,u}^{\text{ph}}=\psi_1^{\text{ph}}\pm\psi_2^{\text{ph}}$. Thus the x-ray photon wave function has certain parity only if the Bragg condition (13) is satisfied. When the Bragg parameter $\mathbf{p}\cdot\mathbf{R}/\pi=$ even or odd the photon wave function $\psi^{\text{ph}}(\mathbf{r})$ is gerade or ungerade, respectively.

A similar decomposition can be written for the high-energy ($kR\gg 1$) Auger electron wave function

$$\psi_{\mathbf{k}}(\mathbf{r})\propto e^{i\beta}(\psi_{\mathbf{k}1}+e^{i\mathbf{k}\cdot\mathbf{R}}\psi_{\mathbf{k}2}). \tag{23}$$

Here $\beta=\mathbf{k}\cdot\mathbf{R}_1$. However, the physical reasons leading, in particular conditions, to a definite parity of $\psi_{\mathbf{k}i}$ are different. Now the effective radius of localization of the Auger orbital $\psi_{\mathbf{k}i}=\psi_{\mathbf{k}i}(\mathbf{r}-\mathbf{R}_i)$ is the wavelength of the Auger electron $\lambda=2\pi/k$. Due to the oscillations of this function in the region $|\mathbf{r}-\mathbf{R}_i|>\lambda$, the corresponding contribution to the decay amplitude can be neglected. In other words, we can consider $\psi_{\mathbf{k}i}\simeq 0$ for $|\mathbf{r}-\mathbf{R}_i|>\lambda$. It should also be noted that the Auger orbital enters in the two Coulomb integrals $g_{\mathbf{k}}$ and $\overline{g_{\mathbf{k}}}$ of Eq. (7). The first, one-center integral will, in general, give the largest contribution and contains, as well as the dipole-matrix element, the core orbital, which then acts as a cutoff in the region a_{1s}.

Contrary to the case of the photon, where we could assume $pa_{1s}\ll 1$, the Auger electron wave function has no definite parity even close to the atom. The expansion of $\psi_{\mathbf{k}i}$ over spherical harmonics $Y_{\text{lm}}(\hat{\mathbf{r}}_i)$ shows that $\psi_{\mathbf{k}i}$ is the sum of contributions of opposite parity [Eq. (9)]. By the properties of these even and odd contributions relative to the inversion at the molecular center, $I\psi_{\mathbf{k}1}^{\text{even}}=\psi_{\mathbf{k}2}^{\text{even}}$, $I\psi_{\mathbf{k}1}^{\text{odd}}=-\psi_{\mathbf{k}2}^{\text{odd}}$, one can construct gerade and ungerade wave functions

$$\psi_{\mathbf{k}}^{g,u}(\text{even}) = \psi_{\mathbf{k}1}^{\text{even}} \pm \psi_{\mathbf{k}2}^{\text{even}}, \quad \psi_{\mathbf{k}}^{g,u}(\text{odd}) = \psi_{\mathbf{k}1}^{\text{odd}} \mp \psi_{\mathbf{k}2}^{\text{odd}}. \tag{24}$$

The item of special interest is the representation of the electron continuum wave function (23) in terms of these functions of certain parity,

$$\psi_{\mathbf{k}}(\mathbf{r}) \propto e^{i(\beta+\mathbf{k}\cdot\mathbf{R}/2)}\left[\cos\left(\frac{\mathbf{k}\cdot\mathbf{R}}{2}\right)\{\psi_{\mathbf{k}}^{g}(\text{even})+\psi_{\mathbf{k}}^{u}(\text{odd})\}\right.$$
$$\left. - i\,\sin\left(\frac{\mathbf{k}\cdot\mathbf{R}}{2}\right)\{\psi_{\mathbf{k}}^{u}(\text{even})+\psi_{\mathbf{k}}^{g}(\text{odd})\}\right]. \tag{25}$$

One can see directly that because of the mixture of even and odd states, the Auger electron wave function has no definite parity in the general case. However, if we assume, as we do in the present investigation, that the MO's ψ_l and ψ_j are π orbitals with negligibly small contribution of d orbitals, then only $\psi_{\mathbf{k}i}^{\text{even}}$ [Eq. (10)] contributes to the Coulomb integrals (7). This means that one can ignore the odd functions $\psi_{\mathbf{k}}^{g}(\text{odd})$ and $\psi_{\mathbf{k}}^{u}(\text{odd})$ in Eq. (25) with the final result

$$\psi_{\mathbf{k}}(\mathbf{r}) \propto e^{i(\beta+\mathbf{k}\cdot\mathbf{R}/2)}\left[\cos\left(\frac{\mathbf{k}\cdot\mathbf{R}}{2}\right)\psi_{\mathbf{k}}^{g}(\text{even})\right.$$
$$\left. - i\,\sin\left(\frac{\mathbf{k}\cdot\mathbf{R}}{2}\right)\psi_{\mathbf{k}}^{u}(\text{even})\right]. \tag{26}$$

When the Bragg parameter $\mathbf{k}\cdot\mathbf{R}/\pi =$ even or odd the Auger electron wave-function is gerade or ungerade, respectively.

Let us now go back to the selection rules. Both representations (22) and (26) show that the photon and Auger electron wave functions have well-defined parities only under the Bragg conditions (13) and (16). One can see immediately that Eqs. (19), (22), and (26) yield the previously derived selection rules [Eq. (17)].

1. Angular distributions of the Auger electron parity and the RAS cross section

As a final comment in this section we point out that the angular dependence of the gerade or ungerade contributions to the Auger electron wave function observed in Eq. (26) corresponds exactly to the angular dependence of the cross section in Eq. (14). This can be easily seen in the case of soft x-ray radiation [$n=0$ in Eq. (14)]

$$\sigma_{g,u}(\epsilon,\omega) = 2\sigma_o(\hat{\mathbf{R}}_o)w_{u,g}, \quad w_f = \begin{cases} \sin^2\left(\dfrac{\mathbf{k}\cdot\mathbf{R}}{2}\right), & f=u \\ \cos^2\left(\dfrac{\mathbf{k}\cdot\mathbf{R}}{2}\right), & f=g. \end{cases} \tag{27}$$

This representation demonstrates that the angular dependence of the RAS cross section for final states with $f=g,u$ coincides with the angular distribution $w_{\bar{f}}$ of the Auger electron wave function with opposite parity $\bar{f}=u,g$ [Eq. (26)] (see Fig. 2).

IV. EFFECTS OF MOLECULAR DISORDER

Free molecules in gas phase are randomly oriented, but upon adsorption they orient themselves in order to minimize the total energy. The most favorable orientation varies with the coverage and nature of the adsorbate and the substrate. The adsorption systems are classified as either physisorbed or chemisorbed depending on the adsorption strength between molecules and the surface. In physisorption the bonding is week, with adsorption energies in the order of 0.1 eV, whereas chemisorption energies are in the order of 1 eV.

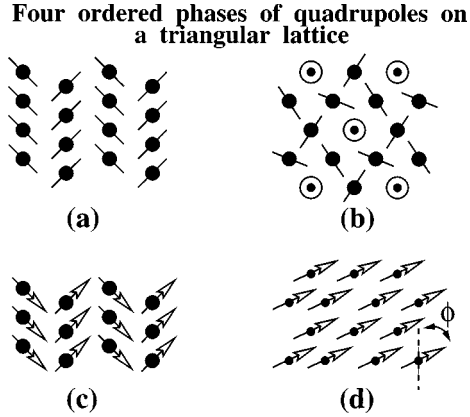

FIG. 3. Four orientationally ordered phases for molecules A_2 physisorbed on a triangular lattice (Ref. 18). (a) Two-sublattice in-plane herringbone phase. (b) Four-sublattice pinwheel phase where the circles with dots indicate the molecules perpendicular to the surface. (c) Two-sublattice out-of-plane herringbone phase. (d) Ferrorotational phase where all molecules are free to rotate uniformly by a constant phase angle ϕ. A systematic out-of-plane tilt of the molecular axes is shown by arrows.

In systems with weak adsorbate-substrate interaction, the adsorbate-adsorbate interaction may be of importance, depending on the coverage. The richness of the structural phase diagrams of physisorption systems arises from the subtle balance between the corrugation of the substrate potential and the adsorbate-adsorbate interaction[18] (Fig. 3). At low coverage only adsorbate-substrate interaction is important. In the case for N_2/Cu system the N_2 molecules reside preferentially inside potential troughs running parallel to the close-packed Cu rows.[19] As the coverage increases, the molecules can form a monolayer with several orientational phases[18] (Fig. 3).

The degree of disorder evidently depends on the system; we consider here both two- and three-dimensional (2D and 3D) disordering. To avoid unnecessary complications let us average the RAS cross section (14) over molecular orientations only at the Bragg limit (13) and (14) where the important case $n=0$ corresponds to soft x-ray scattering. The result of this averaging is conveniently presented in the following form:

$$\bar{\sigma}_f(\epsilon,\omega) = \bar{\sigma}_o[1-(-1)^n\mathcal{P}_f\chi], \tag{28}$$

which includes an interference or coherent factor χ and the averaged cross section $\bar{\sigma}_o$ defined as

$$\chi = \frac{1}{\bar{\sigma}_o}\langle\sigma_o(\hat{\mathbf{R}})\cos(\mathbf{k}\cdot\mathbf{R})\rangle, \quad \bar{\sigma}_o = \langle\sigma_o(\hat{\mathbf{R}})\rangle. \tag{29}$$

The averaging over molecular orientations (in the substrate plane or in the volume) is denoted here by angular brackets. The deviation of the coherent factor χ from 1 shows the

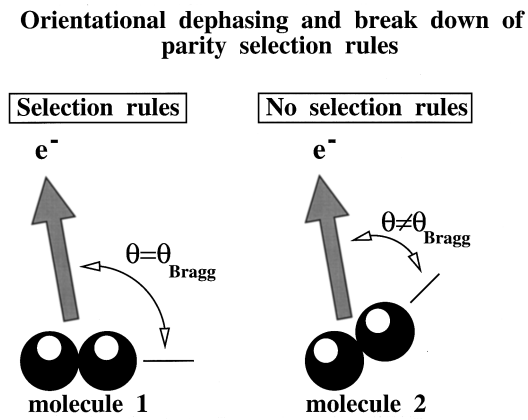

FIG. 4. Qualitative illustration of the orientational dephasing and breakdown of the parity selection rules. According to Eq. (16) the Bragg angle is defined as $\cos\theta_{\mathrm{Bragg}}=n'\pi/kR$.

degree of violation of the parity selection rules (17). The physics of the orientational breakdown of the parity selection rules is shown in Fig. 4.

A. 1D system

The discussion in Secs. II and III concerned only 1D systems, i.e., systems with the same orientation of all molecules; this can be realized, for example, by adsorption on a surface. The axes of the adsorbed molecules can be oriented perpendicular or parallel to the substrate plane. To keep the $D_{\infty h}$ symmetry of homonuclear diatomic molecules the adsorbate-substrate interaction must be small having negligible overlap between adsorbate and substrate valence orbitals and having bonds mediated by weak van der Waals forces. The symmetry relative to the permutation of nuclei can be maintained also for chemisorbed molecules with axes parallel to the surface.

The RAS cross section for 1D systems is given by Eq. (14). To emphasize the qualitative distinction of this strongly ordered case from a disordered system it is worth applying the representation (28) for this case also. Because of the perfect molecular order we have $\overline{\sigma_o}=\sigma_o(\hat{\mathbf{R}})$ and the interference factor (29) now strongly depends on the angle θ between the Auger electron momentum $\mathbf{k}$ and the molecular axis,

$$\chi=\cos(\mathbf{k}\cdot\mathbf{R})=\cos(kR\ \cos\ \theta). \tag{30}$$

To be more specific, let us consider the case of soft x rays ($n=0$). Figure 2 shows the angular dependences of $\overline{\sigma_f}(\epsilon,\omega)$ for gerade and ungerade final states. The cross sections $\overline{\sigma_g}(\epsilon,\omega)$ and $\overline{\sigma_u}(\epsilon,\omega)$ oscillate in opposite phase [see Eq. (27)]. One can clearly see the strict selection rules: $\overline{\sigma_g}(\epsilon,\omega)=0$ for the Bragg angles [Eq. (16)] $\cos\theta_{\mathrm{Bragg}}=2\pi m/kR$, while $\overline{\sigma_u}(\epsilon,\omega)=0$ in the points $\cos\theta_{\mathrm{Bragg}}=\pi(2m+1)/kR$, where m is an integer.

Intuitively, one cannot consider the scattering processes by strictly ordered molecules as independent events. However, this is true only when the intermolecular distances are comparable with the atomic size, i.e., when well-ordered molecules form united electronic bands. In this case the notion of a single molecule is invalid and we indeed have to consider the ensemble of molecules (film or solids) and take into account the coherence of scattering channels through the core excited states localized at different atoms of this united system.[20,21,11] One can say that the x-ray photon and the Auger electron must be considered to be coherently absorbed and emitted, respectively, by the molecular ensemble as a whole. However, when the intermolecular distances are large the valence energy band collapses to a finite set of very narrow bands with energies practically equal to the MO energies of the single molecule A_2. Due to the strong degeneracy of these bands, both the RAS cross section and the amplitude are invariant relative to orthogonal transformations inside the degenerate band. If one transforms the corresponding Bloch states to the MO states localized at different molecules A_2, the RAS cross section reduces to the RAS cross section for a single molecule [Eq. (1)] multiplied by the number of molecules in the system. So we note that our results are valid only for a molecular ensemble with sufficiently large intermolecular distances, i.e., with a negligibly small splitting caused by a weak intermolecular interaction.

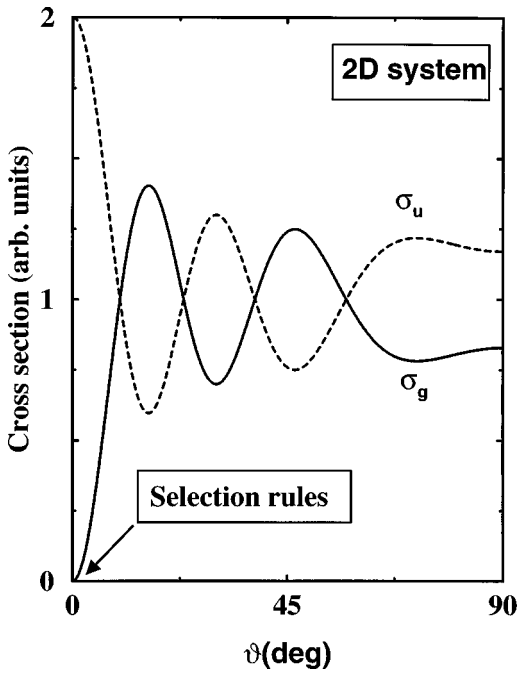

FIG. 5. *2D disorder*. Partial RAS cross section $\overline{\sigma_g}(\epsilon,\omega)$ and $\overline{\sigma_u}(\epsilon,\omega)$ [Eq. (28)] for gerade and ungerade final states, respectively. The case of soft x rays ($n=0$) and chaotical orientation of molecular axes in the substrate plane [Eqs. (31) and (34)]. ϑ is the angle between $\mathbf{k}$ and the surface normal. $kR=14$.

B. 2D system: Molecules adsorbed on a surface

Adsorbed molecules with random orientations of their axes in the surface plane are an example of a partially disordered system. In this case one can expect ''melting'' of the interference pattern [Eqs. (11) and (14)] since the interference fringe is very sensitive to the orientation of the molecular axis relative to the momenta of both the x-ray photon and the Auger electron.

We first consider RAS with a small value of the interference parameter $|\mathbf{k}\cdot\mathbf{R}|\ll 1$. For high-energy Auger electrons this condition is equivalent to ejection of the Auger electron in a direction nearly orthogonal to the surface (see Fig. 5).

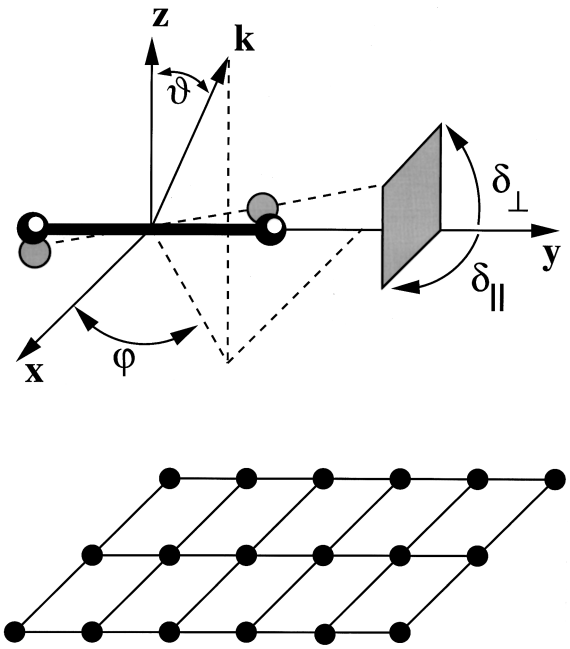

FIG. 6. Geometry of the substrate with physisorbed molecule.

We then have

$$\chi = 1 \quad \text{if } |\mathbf{k}\cdot\mathbf{R}| \ll 1 \quad (\vartheta \simeq 0^o), \tag{31}$$

where ϑ is the angle between the Auger electron momentum $\mathbf{k}$ and the surface normal. The random orientation of the molecular axes in the surface plane does not destroy the parity selection rules for the Auger electrons emitted perpendicular to the surface (Fig. 5). The reason for this is, of course, the small variation of the integrand in Eq. (29) for different molecular orientations.

The detection of the Auger electrons at larger angles ϑ gives a qualitatively different picture. In this case we need to consider explicitly the averaging in Eq. (29), which is now equivalent to the averaging over the angle $\pi/2-\varphi$ between the molecular axis and the plane passing through $\mathbf{k}$ and the surface normal (Fig. 6):

$$\chi = \frac{1}{2\pi\overline{\sigma_o}} \int_0^{2\pi} d\varphi \, \cos(kR \, \sin\vartheta \, \sin\varphi)\sigma_o(\hat{\mathbf{R}}). \tag{32}$$

One can easily obtain this integral in the case of strong oscillations of the integrand due to the large magnitude of the interference parameter

$$|\mathbf{k}\cdot\mathbf{R}| \gg 1 \quad \text{if } |\sin\vartheta| \gg \frac{1}{kR}, \tag{33}$$

a condition that for Auger electron energies around 500 eV and a bond length of 2 a.u. is satisfied already for $\vartheta > 5°$. The main contribution to this integral is given close to the points $\varphi = \pi/2, 3\pi/2$ of stationary phase: $\sin'\varphi = 0$. By making use of the expansion of the trigonometric factor in Eq. (32) in a series of Bessel functions, we obtain

$$\chi = \frac{\sigma_o(\hat{\mathbf{k}}_\parallel)}{\overline{\sigma_o}} J_o(kR \, \sin\vartheta), \quad J_o(x) \simeq \left(\frac{2}{\pi|x|}\right)^{1/2} \cos\left(x - \frac{\pi}{4}\right), \tag{34}$$

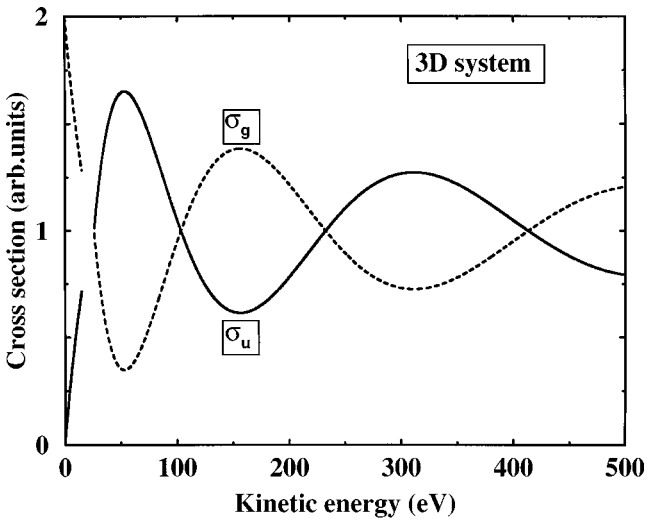

FIG. 7. *3D disorder*. Partial RAS cross section $\overline{\sigma_g}(\epsilon,\omega)$ and $\overline{\sigma_u}(\epsilon,\omega)$ [Eq. (28)] for gerade and ungerade final states, respectively. The case of soft x rays ($n=0$) and chaotical orientation of molecular axes in 3D space [Eq. (36)]. $kR=14$. $\sigma_o(\hat{\mathbf{k}})/\overline{\sigma_o}=3$.

where $\hat{\mathbf{k}}_\parallel$ is the unit vector along the projection of $\mathbf{k}$ on the substrate plane. The asymptotic behavior ($x \ll 1$) of the Bessel function $J_o(x)$ of zero order shows that in contrast to the 1D system (30) the partial disorder of the 2D system suppresses the interference factor by

$$\frac{1}{\sqrt{kR|\sin\vartheta|}} \tag{35}$$

times. The dephasing due to the random orientation of the molecules on the surface plane leads to the breakdown of the parity selection rules (17). However, despite the lowering of the degree of order passing from the 1D to the 2D system, the selection rules (Fig. 5) still apply in the particular case of ejection of the Auger electron perpendicular to the surface.

C. 3D system: Random orientation of surface adsorbates and gas phase molecules

Another relevant case to consider is given by a total random orientation of the molecular axes in 3D space. Clearly, this typical gas phase situation can be realized also for surface adsorbed molecules. One can expect a stronger violation of the parity selection rules in this case, since the degree of 3D disorder is essentially larger than the degree of 2D disorder. Indeed, the averaging of the RAS cross section [Eqs. (28) and (29)] over the angle between $\mathbf{k}$ and molecular axis $\mathbf{R}$ now shows

$$\chi = \frac{\sigma_o(\hat{\mathbf{k}})}{\overline{\sigma_o}} j_o(kR) \quad \text{if } kR \gg 1, \tag{36}$$

with a quenching of the coherence responsible for the selection rules that is faster than for the 2D system because it is now proportional to $1/kR$. Here $j_o(x)=\sin(x)/x$ is the spherical Bessel function of zero order.

Contrary to the 1D and 2D systems, high-energy Auger spectra ($kR \gg 1$) of 3D disordered systems have no parity selection rule (Fig. 7) except for small energies of the Auger

electron $\lesssim 50$ eV when the interchannel coherence is large due to the smallness of the interference parameter, $kR<1$.

For completeness, we will shortly discuss the anisotropic factor $\sigma_o(\hat{\mathbf{k}})/\overline{\sigma_o}$ in expression (36). The anisotropy of the χ function originates in this case from the anisotropy of the photoabsorption and Coulomb factors $(\mathbf{e}\cdot\mathbf{d}_\nu)$ and $g_{\mathbf{k}}$, $\overline{g_{\mathbf{k}}}$, respectively. To clarify the importance of this anisotropy on the interference term let us neglect the anisotropy of the Coulomb decay amplitude. Then it follows that the interference contribution differs in the case of $1s\rightarrow\sigma$ and $1s\rightarrow\pi$ photoabsorption transitions since

$$\frac{\sigma_o(\hat{\mathbf{k}})}{\overline{\sigma_o}}\simeq 3\times\begin{cases}(\mathbf{e}\cdot\mathbf{k})^2 & \text{if } \nu=\sigma\\ \frac{1}{2}(\mathbf{e}\times\mathbf{k})^2 & \text{if } \nu=\pi.\end{cases} \tag{37}$$

In the general case the anisotropy caused by the dependence from $\mathbf{k}$ and $\mathbf{R}$ of the Coulomb integrals $g_{\mathbf{k}}$ and $\overline{g_{\mathbf{k}}}$ must also be taken into account at the right-hand side of this equation.

Figure 7 shows the partial cross sections $\overline{\sigma_g}(\epsilon,\omega)$ and $\overline{\sigma_u}(\epsilon,\omega)$ [Eq. (28)] vs the kinetic energy of the Auger electron for $\sigma_o(\hat{\mathbf{k}})/\overline{\sigma_o}=3$.

V. VIBRATIONAL AND LIBRATIONAL DEPHASING

A. Vibrational dephasing. The anisotropic Debye-Waller factor

Another source of violation of the selection rules is the dephasing factor $\exp(-W)$ multiplying the interference term

$$\chi\rightarrow\chi e^{-W_{\rm vib}}. \tag{38}$$

This is the Debye-Waller (DW) factor, which has the effect of reducing the coherence of all the processes as temperature T increases. Due to the atomic displacement $\mathbf{x}$ the equilibrium internuclear radius-vector $\mathbf{R}$ must be replaced by $\mathbf{R}+\mathbf{x}$. The smallness of this displacement and Eqs. (30), (34), and (36) enable us to see the qualitative difference of the DW factors for 1D, 2D, and 3D systems,

$$W_{\rm vib}=\frac{1}{2}\,k^2\langle x^2\rangle\times\begin{cases}\cos^2\theta, & 1\text{D}\\ \sin^2\vartheta, & 2D\\ 1, & 3\text{D}.\end{cases} \tag{39}$$

The mean-square displacement depends on the vibrational frequency $\omega_{\rm vib}$, the reduced molecular mass μ, and the temperature,

$$\langle x^2\rangle=x_o^2\,\coth\left(\frac{T_{\rm vib}}{2T}\right)=x_o^2\begin{cases}1 & \text{if } T/T_{\rm vib}\ll 1\\ 2T/T_{\rm vib} & \text{if } T/T_{\rm vib}\gg 1.\end{cases} \tag{40}$$

We introduced here the vibrational temperature $T_{\rm vib}$ and the amplitude of the zero-point molecular vibration x_o,

$$T_{\rm vib}=\frac{\omega_{\rm vib}}{k_B},\quad x_o^2=\frac{1}{2\mu\omega_{\rm vib}}, \tag{41}$$

where k_B and μ are the Boltzmann constant and the reduced mass, respectively. Differently from the totally disordered 3D system, the DW factor is strongly anisotropic for 1D and 2D systems. When all the molecules are oriented in the same direction (1D) $W_{\rm vib}$ depends on the angle θ between $\mathbf{k}$ and the molecular axis. $W_{\rm vib}$ depends instead on the angle ϑ between $\mathbf{k}$ and surface normal in the case of a 2D system.

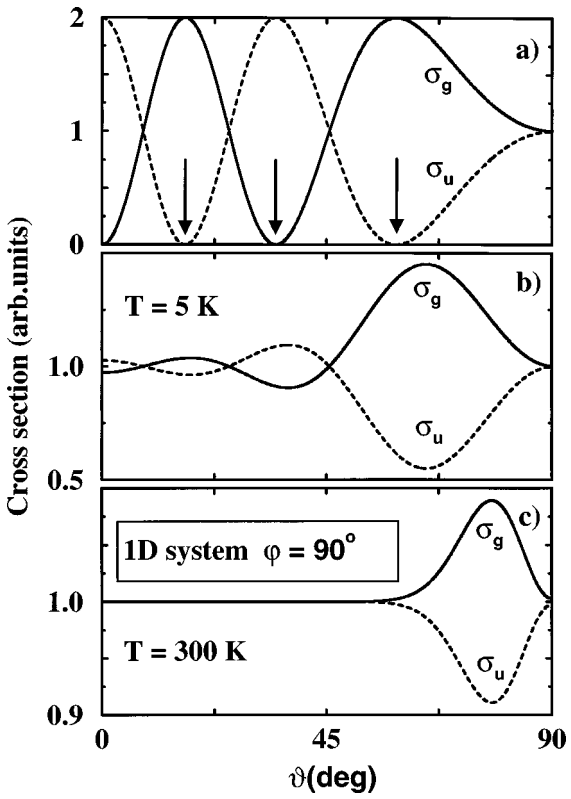

FIG. 8. Role of the librational dephasing on the angular dependence of the RAS cross sections $\overline{\sigma_g}(\epsilon,\omega)$ and $\overline{\sigma_u}(\epsilon,\omega)$ [Eq. (28)] for gerade and ungerade final states, respectively. **1D system**. Input data for the K spectrum of the N_2 molecule: $\epsilon=380$ eV, $T_{\rm lib}\simeq 47.6$ K, $\delta_o=14°$, $kR\simeq 11$ a.u., $\varphi=90°$. (a) No librations, $\delta_o^{(\perp)}=0$. (b) and (c) $\delta_o^{(\perp)}=14°$. The angular dependences of the RAS cross sections are close to case (b) up to $T\simeq 40$ K. The Bragg angles are equal $\vartheta_{\rm Bragg}=0°$, 16.6°, 34.9°, 59.1°.

When the temperature T essentially exceeds the ''vibrational'' temperature $T_{\rm vib}$ the coherence is suppressed. The reason for this violation of the selection rules is the strong dephasing due to thermal excitation of high vibrational states with large amplitude: $(\langle x^2\rangle)^{1/2}\rightarrow x_o(2T/T_{\rm vib})^{1/2}$.

B. Librational dephasing

Surface-adsorbed molecules can be considered perfectly aligned only in a classical physics picture at low temperatures. In reality, zero-point quantum librations of the molecules in their potential wells considerably broaden the orientational distribution. For example, the calculated root-mean-square amplitude of these librations is 14° for the herringbone phase [Fig. 3(a)] of N_2 adsorbed on graphite.[18]

The dephasing caused by the thermal librations results also in a violation of the parity selection rules. Apparently, the effect of librational dephasing is stronger than the vibrational dephasing, due to the weaker van der Waals interaction responsible for the librations. For example, the large librational dephasing for 1D ordered N_2 molecules dominates in comparison with the very small vibrational dephasing, $W_{\rm vib}\simeq 0$ (Fig. 8). The molecular librations in 1D and 2D systems give an additional contribution $W_{\rm lib}$ to the DW factor

$$W=W_{\rm vib}+W_{\rm lib}. \tag{42}$$

To average the χ function (29) over zero-point and thermal librations we consider the density-operator technique

$$\chi=\frac{1}{\overline{\sigma_o}}\ \mathrm{Re\ Tr}[\varrho\,\sigma_o(\hat{\mathbf{R}})e^{i\mathbf{k}\cdot\mathbf{R}}],\quad \varrho=\frac{e^{-\beta H}}{\mathrm{Tr}(e^{-\beta H})},\quad \beta=\frac{1}{k_BT},\tag{43}$$

with H as the libron Hamiltonian and the density operator normalized to unit $\mathrm{Tr}(\varrho)=1$.

We consider first the case of 1D ordering with small librations relative to the equilibrium molecular direction (Fig. 6). In the general case the librations in the surface plane ($\parallel$) and those ''tilted'' out of the plane ($\perp$) have different amplitudes and frequencies. The scalar product $\mathbf{k}\cdot\mathbf{R}$ is then simply written as

$$\mathbf{k}\cdot\mathbf{R}\simeq kR\ \sin\ \vartheta\ \sin\ \varphi+kR(\delta_\perp\cos\ \vartheta+\delta_\parallel\sin\ \vartheta\ \cos\ \varphi).\tag{44}$$

Due to the smallness of librations the density operator factorizes

$$\varrho=\varrho_\perp\varrho_\parallel.\tag{45}$$

The harmonic approximation leads to the well-known expression for the density operator in configuration space[22]

$$\varrho_j(\delta,T)=\frac{1}{\sqrt{2\pi\langle\delta_j^2\rangle}}\exp\left(-\frac{\delta^2}{2\langle\delta_j^2\rangle}\right),\quad j=\perp,\parallel.\tag{46}$$

This immediately results in the following expression for the interference term (43):

$$\chi=\begin{cases}\cos(kR\ \sin\ \vartheta\ \sin\ \varphi)e^{-W}, & \text{1D}\\ \dfrac{\sigma(\hat{\mathbf{k}}_\parallel)}{\overline{\sigma_o}}\,J_o(kR\ \sin\ \vartheta)e^{-(W_{\mathrm{vib}}+W_\perp)}, & \text{2D.}\end{cases}\tag{47}$$

Let us be reminded that the χ function for 2D disorder is written here in the limit (33). This equation can be very approximately extrapolated in the region of small $kR|\sin\vartheta|$ if we replace $\sigma(\hat{\mathbf{k}}_\parallel)/\overline{\sigma_o}$ by 1. Similar to vibrational dephasing the libron DW factor is strongly anisotropic

$$W_{\mathrm{lib}}=W_\perp+W_\parallel,$$

$$W_j=\frac{1}{2}\,k^2R^2\langle\delta_j^2\rangle\times\begin{cases}\cos^2\ \vartheta, & j=\perp\\ \sin^2\ \vartheta\ \cos^2\ \varphi, & j=\parallel.\end{cases}\tag{48}$$

The mean square of libron angles δ_j depends on the temperature and on an amplitude of the zero-point librons $\delta_o^{(j)}$ ($j=\perp,\parallel$),

$$\langle\delta_j^2\rangle=\delta_o^{(j)2}\ \coth\left(\frac{T_{\mathrm{lib}}^j}{2T}\right)=\delta_o^{(j)2}\begin{cases}1 & \text{if } T/T_{\mathrm{lib}}^j\ll 1\\ 2T/T_{\mathrm{lib}}^j & \text{if } T/T_{\mathrm{lib}}^j\gg 1.\end{cases}\tag{49}$$

The libron temperature T_{lib}^j and amplitude of zero-point molecular librations $\delta_o^{(j)}$ depend on the libron frequency $\omega_{\mathrm{lib}}^{\perp,\parallel}$ as

$$T_{\mathrm{lib}}^j=\frac{\omega_{\mathrm{lib}}^j}{k_B},\quad \delta_o^{(j)2}=\frac{1}{2\mu R^2\omega_{\mathrm{lib}}^j},\quad j=\perp,\parallel.\tag{50}$$

The zero-point libron temperature $T_{\mathrm{lib}}^j/2$ is about 25 K for N_2 physisorbed on graphite. It is a good estimation of the temperature of the orientational phase-transition.[18]

The investigations in Refs. 23, 24, 19, and 18 show that tilting and in-plane librations have the same order of magnitude $\delta_o^{(\perp)}\sim\delta_o^{(\parallel)}\sim 10°-20°$. This means that one cannot suppress out-of-plane and in-plane librations simultaneously. It is therefore appropriate to stress that the librational dephasing is never completely absent ($W_{\mathrm{lib}}\neq 0$), and the librations will violate the parity selection rules (given by the ideal 1D system) for all directions of the Auger electron detection, Fig. 8. Such kinds of librations are the result of the large magnitude of the interference parameter kR. For example, for N_2, $kR\simeq 11$ a.u. Let us suppress the in-plane librations choosing $\varphi=90°$ and consider the typical case of large kR. From Eq. (47) it is obvious that the parity selection rules then are approximately fulfilled [Fig. 8(b)] for the large Bragg angles ($\vartheta_{\mathrm{Bragg}}\simeq 59.1°$ in Fig. 8) and low temperature since the DW factor then is small. Another important distinction between an ideal 1D system [Fig. 8(a)] and 1D ordered molecules with the librational degrees of freedom is that the position of the minimum of $\overline{\sigma_u}(\epsilon,\omega)$ [Figs. 8(b) and 8(c)] does not coincide with the Bragg angle [$\vartheta_{\mathrm{Bragg}}\simeq 59.1°$, Fig. 8(a)]. The librational shift of this minimum position is caused by the DW factor (48).

1. Determination of the mean-square libron angles

The libron suppression of the parity-selection rules can be used for the experimental measurements of the mean-square amplitudes of out-of-plane and in-plane librations. We describe here one method on how to accomplish this. The vibrational DW factor W_{vib} is small in a broad temperature region and can be neglected. The mean-square tilting and in-plane angles $\langle\delta_\perp^2\rangle$ and $\langle\delta_\parallel^2\rangle$ can be found from experimental data as

$$\langle\delta_j^2\rangle=\frac{2}{(kR)^2}\ln\frac{1}{\xi},\quad \frac{\overline{\sigma_u^{\mathrm{Bragg}}}(\epsilon,\omega)}{\overline{\sigma_u^0}(\epsilon,\omega)}=\frac{1-\xi^\tau}{1+\xi},\tag{51}$$

where ξ is the solution of the latter equation and

$$\tau=\begin{cases}\cos^2\vartheta_{\mathrm{Bragg}}\\ \cos^2\varphi_{\mathrm{Bragg}},\end{cases}$$

$$\frac{\pi(2m+1)}{kR}=\begin{cases}\sin\vartheta_{\mathrm{Bragg}} & \text{if } j=\perp,\ \varphi=90°\\ \sin\varphi_{\mathrm{Bragg}} & \text{if } j=\parallel,\ \vartheta=90°,\end{cases}\tag{52}$$

with integer $m\geqslant 0$. These equations follow from Eqs. (28), (47), and (48) for 1D ordering. To determine $\langle\delta_\perp^2\rangle$ we need to choose $\varphi=90°$ and to measure the RAS cross sections $\overline{\sigma_u^0}(\epsilon,\omega)$ and $\overline{\sigma_u^{\mathrm{Bragg}}}(\epsilon,\omega)$ for $\vartheta=0°$ and $\vartheta=\vartheta_{\mathrm{Bragg}}$, respectively (Fig. 6). The in-plane detection of Auger electrons ($\vartheta=90°$) for two azimuthal angles $\varphi=0°$ and $\varphi=\varphi_{\mathrm{Bragg}}$ allows us to measure $\overline{\sigma_u^0}(\epsilon,\omega)$ and $\overline{\sigma_u^{\mathrm{Bragg}}}(\epsilon,\omega)$ and to determine the mean-square angle $\langle\delta_\parallel^2\rangle$. The case of physisorbed N_2 molecules shown in Fig. 8 says that the parameter $(kR\tau)^2$ is generally large due to the large energy of the Auger electron. The procedure of extraction of $\langle\delta_j^2\rangle$ from experimental data is simpler in this case,

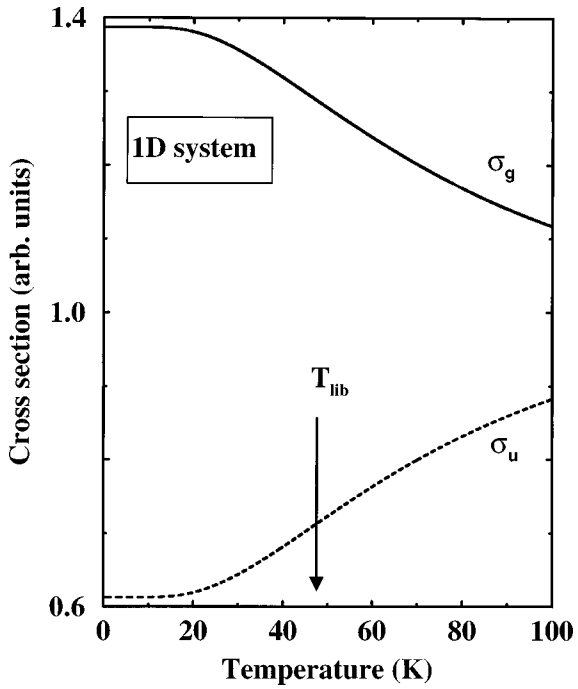

FIG. 9. Zero-point and thermal dephasing for the 1D case. The breaking of the parity selection rules $[\overline{\sigma_u}(\epsilon,\omega)\neq 0]$ near $T=0$ K are caused mainly by the zero-point molecular librations. $\vartheta=\vartheta_{\mathrm{Bragg}}=59.1°$. The input data for the K spectrum of the N_2 molecule are the same as for Fig. 8.

$$\langle \delta_j^2\rangle = \frac{2}{(kR\tau)^2}\ln\frac{\overline{\sigma_u^0}(\epsilon,\omega)}{\overline{\sigma_u^0}(\epsilon,\omega)-\overline{\sigma_u^{\mathrm{Bragg}}}(\epsilon,\omega)}, \quad (kR\tau)^2\gg 1. \tag{53}$$

Since librations strongly quench the interference fringe [Figs. 8(b) and 8(c)] the Bragg angles $\vartheta_{\mathrm{Bragg}}$ (or φ_{Bragg}) [Eqs. (52)] must be chosen close to 90° where W_{lib} is smallest.

C. Role of the zero-point vibrations and librations

In contrast to the classical view the ''thermal'' quenching of coherence (38) does not disappear when $T\to 0$ since $\langle x^2\rangle\to x_o^2\neq 0$ [Eq. (40)] and $\langle\delta_j^2\rangle\to\delta_o^{(j)2}$ [Eq. (49)] [Fig. 8(b)]. The dephasing at zero temperature is caused by the zero-point vibrations and librations with amplitudes x_o and $\delta_o^{(j)}$, respectively. As one can see from Eq. (48) and Fig. 8 the librational dephasing is never completely absent. Figure 8 shows that zero-point librations violate the parity selection rules $[\overline{\sigma_{g,u}}(\epsilon,\omega)\neq 0]$ even for zero temperature. The vibrational dephasing in the case of N_2 is negligibly small in the considered temperature region $W_{\mathrm{vib}}\simeq 0$. Figures 8 and 9 show that the thermal librations lead to the ''melting'' of the interference pattern when $T>T_{\mathrm{lib}}$.

We analyzed in this section only the DW factor caused by electron momentum **k**. Apparently, the thermal dephasing suppresses also the coherence associated with the photon momentum **p** [see Eq. (11)]. We did not take this effect, important for hard x-ray radiation, into account.

D. The role of electron-phonon interaction

The violation of parity-selection rules can be also due to another effect quite typical for core excited states of symmetrical molecules, namely, the electron-phonon interaction mixing close-lying electronic states of different parity. Such quasi-Jahn-Teller effects[25,26] are not possible in free A_2 molecules. However, the electron-phonon violation of selection rules may become important when the molecules are chemisorbed. The effect can be suppressed by detuning the x-ray photon frequency from the photoabsorption resonance.[27,26]

VI. ROLE OF AUGER ELECTRON DIFFRACTIONAL SCATTERING

X-ray photoelectron diffraction and Auger electron diffraction (AED) effects have been studied for a long time.[28–30] Both effects constitute surface-structural probes sensitive to short-range order. The physical reason behind the diffractional oscillations of the photoelectron and Auger electron yields is the diffractional scattering of the electron ejected by adsorbate on the surrounding atoms. The basis of both effects is the same as for extended x-ray-absorption fine structure.[31] The AED effect can mask the interference effect discussed here. Therefore, one needs to understand the possibilities of selecting the signal of interest from the AED oscillations.

The high-energy wave function (3) neglects the scattering of Auger electron by surrounding atoms and describes the main effect of interest. We consider the AED effect using the *muffin-tin* (MT) or Korringa-Kohn-Rostoker approximation as a starting point.[15] We favor this technique because of its simplicity and accuracy for high-energy electrons. The MT method allows us to obtain the following high-energy asymptote for the Auger electron wave function (3) inside the MT sphere of the ith atom of the A_2 molecule:[16–32]

$$\psi_{\mathbf{k}}(\mathbf{r}) = e^{i\mathbf{k}\cdot\mathbf{R}_i}\Bigg(\psi_{\mathbf{k}i}+\sum_{j(\neq i)}\frac{\exp[i(kR_{ij}-\mathbf{k}\cdot\mathbf{R}_{ij})]}{R_{ij}} \times f_j(\Theta_{ij\mathbf{k}})\psi_{\mathbf{k}_{ij}i}\Bigg), \tag{54}$$

where $\mathbf{k}_{ij}=k\hat{\mathbf{R}}_{ij}$, $\mathbf{R}_{ij}=\mathbf{R}_i-\mathbf{R}_j$, $\cos(\Theta_{ij\mathbf{k}})=(\hat{\mathbf{R}}_{ij}\cdot\mathbf{k})$, $\cos(\Theta_{ijn})=(\hat{\mathbf{R}}_{ij}\cdot\hat{\mathbf{R}}_{jn})$ $\psi_{\mathbf{k}i}=\psi_{\mathbf{k}i}(\mathbf{r}-\mathbf{R}_i)$ is the solution of the Schrödinger equation inside of the ith MT sphere without account of scattering by surrounding atoms. The renormalized scattering amplitudes $f_j(\Theta_{ij\mathbf{k}})$ of the Auger electron by the jth scatterer at the angle $\Theta_{ij\mathbf{k}}$ between vectors **k** and $\mathbf{R}_{ij}$ satisfy the equations

$$f_j(\Theta_{ij\mathbf{k}}) = f_j^0(\Theta_{ij\mathbf{k}})+\sum_{m(\neq j)} f_j^0(\Theta_{ijm})\frac{e^{i(kR_{jm}-\mathbf{k}\cdot\mathbf{R}_{jm})}}{R_{jm}} \times f_m(\Theta_{jmk}). \tag{55}$$

A perturbative solution of this equation leads to the multiple-scattering (MS) expansion. Since this scattering is weak for high-energy electrons, the MS expansion converges rapidly. Hence, the renormalized scattering amplitude is very close to the scattering amplitude $f_j^0(\Theta_{ij\mathbf{k}})$ for single scatterer j, except in the case of forward scattering. Strictly speaking, the corresponding MS amplitude diverges for forward scattering due to the large amplitude $f_j(0)$. This can result in self-channeling of the forward-scattered Auger electrons.[30]

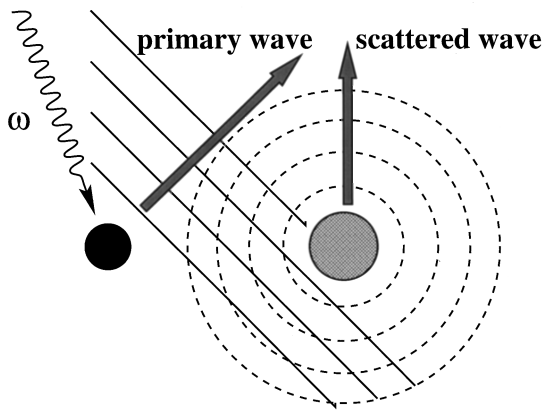

FIG. 10. Physical picture of the Auger electron diffractional scattering by surrounding atoms.

The first term on the right-hand side of Eq. (54) coincides with the primary wave (3) while the second one takes into account the multiple scattering of Auger electrons by the surrounding (Fig. 10). The AED intensity modulations are caused by the interference of the primary electron-electron waves $\psi_{\mathbf{k}i}\exp(i\mathbf{k}\cdot\mathbf{R}_i)$, which originate at the emitter i, and the secondary or scattered electron wave given by the second term on the right-hand side of Eq. (54) (Fig. 10). This oscillatory term leads to dephasing, and hence to a suppression of the interference contribution χ [Eq. (29)]. Thus multiple-scattering corrections can also lead to violations of the parity selection rules. One can easily evaluate the RAS cross section with the wave function of Auger electron in Eq. (54). However, since the final expression is rather complex we restrict ourselves only to a qualitative analysis of AED.

Since AED leads also to oscillatory structure of the RAS cross section we need to understand when AED is large and when this effect can be neglected. As one can see from Eq. (54) the magnitude of the AED modulation mainly depends on the atomic-scattering amplitude $f_j(\Theta)$, which is strongly anisotropic for high-energy electrons;[16,30] starting from a large value $f_j(0)$, $f_j(\Theta)$ decreases rapidly as Θ increases. The magnitude of $f_j(\Theta)$ is very atomic sensitive; the scattering strength is small for light elements and increases with the atomic number. To be more specific, we consider molecules adsorbed parallel to the surface. The AED modulation is then large for forward scattering, i.e., when the Auger electrons are detected in a direction parallel to substrate. The amplitude of the AED oscillations can be, in this case, as large as 70%.[30] These oscillations are rapidly quenched for detection at a large angle between $\mathbf{k}$ and $\mathbf{R}$. For example, the anisotropy or oscillation amplitude decreases from $\sim 24\%$ at $\Theta = 7°$ to $\sim 6\%$ at $\Theta = 45°$ for the system O/Cu(001) (Ref. 28) (here Θ is the angle between $\mathbf{k}$ and the surface plane).

We can then conclude that the AED effect can be neglected here for high-energy Auger electrons ($\epsilon \gtrsim 500$ eV) if the direction of detection is not close to the surface plane.

VII. POSSIBILITY OF EXPERIMENTAL OBSERVATIONS

A few words about the possibility of experimental observation of the parity selection rules and the interference oscillation vs order of the system are relevant. An important aspect is the choice of the molecular system; the interaction of the molecule with the substrate can reduce the symmetry of the isolated molecule, as, for instance, when an A_2 molecule adsorbs perpendicular to the surface with a relatively strong interaction. It is then desirable to have a physisorbed phase instead of a chemisorbed one. Physisorbed up or down phases can be experimentally prepared by dosing molecules at the temperature of liquid helium (25 K) as described in Ref. 12 for a monolayer of O_2 physisorbed on different substrates [Pt(111), Ag(110), and graphite]. The Auger experiments with O_2 (Ref. 12) and with N_2 physisorbed on graphite[33] describe the conditions to check practically the parity-selection rules for these molecules.

Another experimental requirement is the possibility of detecting the Auger electron at different angles; this is a technique already available.[6] In order to enhance the surface sensitivity it will be necessary to use exciting radiation incident on the sample at a small grazing angle (3°–5°). On the other hand, the detection of the Auger electrons close to the direction of the molecular axis is not desirable due to the strong AED effect (see Sec. VI).

A favorable experimental arrangement would thus be given by grazing irradiation of molecules adsorbed perpendicular to the surface with the detection direction far from the surface normal (1D system) or grazing irradiation of molecules adsorbed parallel to the surface with the detection direction perpendicular to the substrate (2D system).

VIII. SUMMARY

Systems with equivalent atoms are very specific for x-ray radiative Raman scattering owing to the interference of the scattering channels through core excited states localized at different atoms.[34,20,9,21,35–38,11] The present investigation on resonant Auger scattering of surface-adsorbed and gas-phase molecules gives another example of this effect, predicting that the RAS cross section can show oscillations caused by the interference of both photon and Auger electron wave functions. We found parity selection rules in the RAS process involving π valence MO's in the Auger decay. Special attention was paid to surface-adsorbed molecules and how the selection rules may be used to investigate the degree of orientational disorder of the system. Indeed, the results of Sec. IV indicate that the dependence of the RAS cross section on the detection angle of the Auger electron is qualitatively different for one-, two-, and three-dimensional systems. Totally ordered molecules (1D system) obey parity selection rules in the soft x-ray region for a set of detection angles corresponding to even or odd values of the Bragg parameter $(\mathbf{k}\cdot\mathbf{R})/\pi$. Contrary to the 1D system the parity selection rules for the 2D system (disordered molecules lying flat on a surface) take place only when the Auger electron is detected perpendicular to the substrate. The selection rules are instead practically absent in the case of totally disordered 3D systems like gas-phase molecules. The reason for this different behavior is the orientational dephasing of the coherent phase sensitive contribution to the RAS cross section.

Different mechanisms leading to the breakdown of the selection rules have been considered; the dephasing caused by molecular vibrations and librations was found to be such a mechanism. We found that the probability of violation of the parity selection rules increased with temperature, but that

even for zero temperature there may be a partial breakdown due to the zero-point vibrations and librations. The librational dephasing dominates in the case of physisorbed molecules. A method for experimental measurement of the mean-square angles of tilting and in-plane librations was suggested.

ACKNOWLEDGMENTS

This work was supported by the Swedish National Research Council (NFR) and the Italian National Research Council (CNR).

*Permanent address: Institute of Automation and Electrometry, 630090 Novosibirsk, Russia.

[1] J. Nordgren, J. Electron Spectrosc. Relat. Phenom. **78**, 25 (1996).

[2] T. Åberg and B. Crasemann, in *Resonant Anomalous X-Ray Scattering. Theory ad Applications*, edited by G. Materlik, C. J. Sparks, and K. Fischer, (North-Holland, Amsterdam, 1994), p. 431.

[3] P. L. Cowan, in *Resonant Anomalous X-Ray Scattering. Theory and Applications* (Ref. 2), p. 449.

[4] W. Eberhardt, in *Applications of Synchrotron Radiation*, Springer Series in Surface Sciences edited by W. Eberhardt Vol. 35 (Springer-Verlag, Berlin, 1995), p. 203.

[5] P. P. Kane, Radiat. Phys. Chem. **50**, 31 (1997).

[6] N. Mårtensson, in *Applications of Synchrotron Radiation* (Ref. 4), p. 65.

[7] A. Nilsson, M. Weinelt, T. Wiell, P. Bennich, O. Karis, N. Wassdahl, J. Stöhr, and M. Samant, Phys. Rev. Lett. **78**, 2847 (1997).

[8] M. Weinelt, A. Nilsson, M. Magnuson, T. Wiell, N. Wassdahl, O. Karis, A. Föhlisch, N. Mårtensson, J. Stöhr, and M. Samant, Phys. Rev. Lett. **78**, 967 (1997).

[9] F. Gel'mukhanov and H. Ågren, Phys. Rev. A **49**, 4378 (1994).

[10] Y. Luo, H. Ågren, and F. Gel'mukhanov, J. Phys. B **27**, 4169 (1994).

[11] F. Gel'mukhanov and H. Ågren, Phys. Rev. B **57**, 2780 (1998).

[12] O. Karis, B. Hernnäs, C. Puglia, A. Nilsson, N. Mårtensson, D. Edvardsson, and S. Lunell, Surf. Sci. **352–354**, 511 (1996).

[13] V. Carravetta, F. Kh. Gel'mukhanov, H. Ågren, S. Sundin, S. J. Osborne, A. Kikas, O. Björneholm, A. Ausmees, and S. Svensson, Phys. Rev. A **56**, 4665 (1997).

[14] H. Ågren, A. Cesar, and C.-M. Liegener, Adv. Quantum Chem. **23**, 1 (1992).

[15] J. Stöhr, *NEXAFS Spectroscopy* (Springer-Verlag, Berlin, 1992).

[16] L. N. Mazalov, F. Kh. Gel'mukhanov, and V. M. Chermoshentsev, J. Struct. Chem. **15**, 975 (1975).

[17] J. L. Dehmer and D. Dill, in *Electron-Molecule and Photon-Molecule Collisions*, edited by T. Rescigno, V. McKoy, and B. Schneider (Plenum, New York, 1979).

[18] D. Marx and H. Wiechert, Adv. Chem. Phys. **95**, 213 (1996).

[19] A. Marmier, C. Ramseyer, P. N. M. Hoang, C. Girardet, J. Goerge, P. Zeppenfeld, M. Büchel, R. David, and G. Comsa, Surf. Sci. **383**, 321 (1997).

[20] F. Gel'mukhanov, L. N. Mazalov, and N. A. Shklyaeva, Zh. Eksp. Teor. Fiz. **71**, 960 (1976) [Sov. Phys. JETP **44**, 504 (1977)].

[21] Y. Ma, K. E. Miyano, P. L. Cowan, Y. Aglizkiy, and B. A. Karlin, Phys. Rev. Lett. **74**, 478 (1995).

[22] R. P. Feynman, *Statistical Mechanics: A Set of Lectures* (Benjamin, Reading, MA, 1972).

[23] S. E. Roosevelt and L. W. Bruch, Phys. Rev. B **41**, 12 236 (1990).

[24] K. B. K. Tang, J. Villette, D. Teillet-Billy, J. P. Gauyacq, and R. E. Palmer, Surf. Sci. **368**, 43 (1996).

[25] L. S. Cederbaum, J. Chem. Phys. **103**, 562 (1995).

[26] A. Cesar, F. Gel'mukhanov, Y. Luo, H. Ågren, P. Skytt, P. Glans, J.-H. Guo, K. Gunnelin, and J. Nordgren, J. Chem. Phys. **106**, 3439 (1997).

[27] P. Skytt, P. Glans, J.-H. Guo, K. Gunnelin, J. Nordgren, F. Gel'mukhanov, A. Cesar, and H. Ågren, Phys. Rev. Lett. **77**, 5035 (1996).

[28] H. Siegbahn and L. Karlsson, in *Photoelectron Spectroscopy of Atoms, Molecules, and Condensed Matter. Handbuch der Physik*, edited by W. Melhorn (Springer-Verlag, Berlin, 1982), Vol. 31.

[29] C. S. Fadley, Surf. Sci. Rep. **19**, 231 (1993).

[30] G. Granozzi and M. Sambi, in *Chemisorption and Reactivity on Supported Clusters and Thin Films: Towards an Understanding of Microscopic Processes in Catalysis*, edited by R. M. Lambert and G. Pacchioni (Kluwer, Academic, Dordrecht, 1997), p. 237.

[31] P. A. Lee, P. H. Citrin, P. Eisenberger, and B. M. Kincaid, Rev. Mod. Phys. **53**, 769 (1981).

[32] F. Gel'mukhanov and H. Ågren, Phys. Rev. B **50**, 11 121 (1994).

[33] H. Tillborg, A. Nilsson, B. Hernnäs, N. Mårtensson, and R. E. Palmer, Surf. Sci. **295**, 1 (1993).

[34] F. Gel'mukhanov, L. N. Mazalov, and N. A. Shklyaeva, Zh. Eksp. Teor. Fiz. **69**, 1971 (1975) [Sov. Phys. JETP **42**, 1001 (1975)].

[35] F. Gel'mukhanov and H. Ågren, J. Phys. B **29**, 2751 (1996).

[36] P. Glans, K. Gunnelin, P. Skytt, J.-H. Guo, N. Wassdahl, J. Nordgren, H. Ågren, F. Gel'mukhanov, T. Warwick, and E. Rotenberg, Phys. Rev. Lett. **76**, 2448 (1996).

[37] P. Glans, P. Skytt, K. Gunnelin, J.-H. Guo, and J. Nordgren, J. Electron Spectrosc. Relat. Phenom. **82**, 193 (1996).

[38] J. D. Mills, J. A. Sheehy, T. A. Ferrett, S. H. Southworth, R. Mayer, D. W. Lindle, and P. W. Langhoff, Phys. Rev. Lett. **79**, 383 (1997).